Supporting Information

Børud et al. 10.1073/pnas.1103321108

SI Materials and Methods

Bacterial Strains and Culture Conditions. The bacterial strains used in this study are described in Table 1 and were grown on conventional GC medium as described previously (1). Protein glycosylation mutations (*pglA, pglC, pglE*$_{on}$, *pglI*) were introduced into various strain backgrounds by using transformation as previously described (2, 3). Construction of the different *pglH* mutant strains is described later. The N400 *galE* mutants were made by transformation with MS11 *galE::cat* genomic DNA (4). The pPilE::*cat* plasmid was used to inactivate the WT *pilE* locus (5). Antibiotics were used for selection of transformants at the following concentrations: streptomycin, 750 μg/mL; erythromycin, 8 μg/mL; kanamycin, 50 μg/mL; and chloramphenicol, 10 μg/mL.

Allelic Exchange of the *pgl* Locus. The introduction of ST-640, FA1090, Z2491, and FAM18 *pgl* loci into N400 were performed through a two-step mutagenesis strategy that allowed gene replacement without introducing any selectable marker into the final strain (Fig. S1). The method uses a two-gene cassette containing both a selectable marker (*ermC′*) and a counter-selectable marker (*rpsL*$^+$) (6). Genomic DNA from the strain of interest was then inserted into N400 by homologous recombination that replaced the *ermC′/rpsL*$^+$ cassette with the *pgl* locus from the strain of interest, and the final strain could be selected on streptomycin plates (7).

Construction of *pglH* Mutants. First, a pCRII-*pglH* plasmid was constructed by PCR-amplifying the whole *pglH* gene and surrounding sequences (2,523 bp) from FA1090 (*pglH* primers, forward, 5′-TCTGAATCAAGCGCGTCGCG-3′; reverse, 5′-TATCTGGCAGGCTGCATCCT-3′) and inserting the PCR product into the pCRII-TOPO vector (Invitrogen). The *pglH* insert was cut out with *Eco*RI and ligated into the pUP6 *Eco*RI site, resulting in pUP6-*pglH*. Then, the *ermC′/rpsL*$^+$ cassette from pFLOB4300 was amplified (pUC primers, forward, MluI, 5′-CCGACGCGTCCCAGTCACGACGTTGTAAAACG-3′; reverse, MluI, 5′-CCGACGCGTAGCGGATAACAATTTCACACAGG-3′), and subsequently cloned into the *Mlu*I sites in pUP6-*pglH* plasmid, resulting in the pUP6-*pglH::ermC′/rpsL*$^+$ plasmid. Gonococci were then transformed with pUP6-*pglH::ermC′/rpsL*$^+$ and erythromycin-resistant *pglH* mutants were selected.

To introduce the H371R mutation into the endogenous site of *pglH*$_{FA1090}$, the pCRII-*pglH* plasmid was mutated by using the specific primers containing the mutation (BP112, 5′-CGCCGCTTCAGGC**G**CGACATTTCCTATCG-3′/BP113, 5′-CGATAGGAAATGTC**G**C**G**CCTGAAGCGGCG-3′) and the QuikChange XL Site-Directed Mutagenesis Kit (Agilent Technologies) as described in the manual. The mutation was then introduced into the FA1090 *pglH* strains by homologous recombination that replaced the *ermC′/rpsL*$^+$ cassette with *pglH*$_{FA1090\ H371R}$ from pCRII-*pglH*$_{FA1090\ H371R}$.

Complementation Analysis. The *pglH*$_{FA1090}$ gene was amplified with specific primers (BP102, 5′-CCTTAATTAAATGAACATTACCATAGCCGC-3′; BP103, 5′-CCAATGCATCTCATTTGCCAATCTTTCAA-3′) containing *Nsi*I and *Pac*I restriction sites, and subcloned into the plasmid pGCC6, digested with *Nsi*I and *Pac* I. The *pglH* gene from FA1090 was there inserted at an intergenic chromosomal site located between the *lctP* and *aspC* genes and linked to a chloramphenicol resistance cassette (8, 9) in the pGCC6::*pglH*$_{FA1090}$ plasmid. To do complementation analysis, this plasmid was then transformed into gonococci and selected on plates containing chloramphenicol. Additionally, pGCC6::*pglH*$_{FAM18}$ (BP104, 5′-CCTTAATTAAATGAACATTACCATCGTCGC-3′; BP105, 5′-CCAATGCATTTCATGAGCTAATCTTTCAA-3′), pGCC6::*pglH*$_{Z2491}$ (BP100, 5′-CCTTAATTAAATGAACATCACCATAGTCGC-3′; BP105), and pGCC6::*pglH*$_{ST640}$ (BP100/BP101, 5′-CCAATGCATTTCATCAGCTAATCTTTCAA-3′) were constructed and transformed into gonococci by using the same approach. Introduction of mutations into pGCC6::*pglH*$_{FA1090\ H371R}$ (BP112/BP113), pGCC6::*pglH*$_{FAM18\ R373H}$ (BP118, 5′-CGCCGCTTCAAACACGACGTTGCCTATC-3′; BP119, 5′-GATAGGCAACGTCGTGTTTGAAGCGGCG-3′), pGCC6::*pglH*$_{Z2491\ R371H}$ (BP116, 5′-CGCCGCTTCAGGCACGACATTTCCTAT-3′; BP117, 5′-ATAGGAAATGTCGTGCCTGAAGCGGCG-3′), and pGCC6::*pglH*$_{ST640\ R373H}$ (BP118/BP119) was performed by using the specific primers with the mutation (shown in parents) and the QuikChange XL Site-Directed Mutagenesis Kit (Agilent Technologies) as described in the manual.

Monosaccharide Analysis. The samples were subjected to methanolysis with 4 M HCl in anhydrous MeOH for 24 h at 80 °C (10, 11). Mannitol was used as an internal standard. After the methanolysis, the reagents were removed under a stream of N_2, and the methyl glycosides were dried in vacuum over P_2O_5 for at least 1 h before conversion into the corresponding trimethylsilyl derivates. The samples were subjected to capillary gas chromatography (6000 Vegas Series 2; Carlo Erba) as described previously (11).

Development of Glycan-Specific Rabbit Polyclonal Antibodies. Polyclonal antibodies (pDAb2 and pGAb2) were generated by rabbit immunization by using pili purified from the strain N400 *pgl*$_{Z2491}$ *pglA* or N400 *pgl*$_{FAM18}$ *pglA* that expresses the protein-linked PglH made diNAcBac or GATDH disaccharides, respectively (Agrisera). Solid-phase affinity purification was done by immunoblotting a whole-cell lysate from the strain expressing the respective glycan and incubating with pDAb2 or pGAb2 (1:2,000 dilutions).

Protein Expression and Purification. *PglH* from *N. meningitidis* strain Z2491 was amplified by PCR and inserted into *Bam*HI/*Xho*I in the pMAL-c2X vector. This construct encoded for the addition of an N-terminal MBP. PglH was heterologously overexpressed in the *E. coli* BL21-Gold (DE3) strain (Agilent). An overnight culture of cells was prepared, and 5 mL was used to inoculate 1 L of Luria–Bertani media at 37 °C with shaking. After the cells reached an optical density of approximately 0.8 absorbance units, the temperature was lowered to 16 °C and the cells were induced with 0.5 mM IPTG. After growth for 16 to 18 h with shaking, the cells were harvested and the pellets were stored at −80 °C.

The glycosyltransferase PglH was expressed as a MBP fusion protein, and this tag was used to purify the protein by using amylose resin (New England Biolabs). A 1-L cell pellet was solubilized in 40 mL of buffer containing 50 mM Tris (pH 8.0), 150 mM NaCl, and 5% glycerol, and then lysed by sonication. The lysate was cleared by centrifugation (145,000 × *g*) for 65 min at 4 °C. Cleared lysate was mixed with 2 mL of amylose resin and tumbled for 30 min at 4 °C and then packed into a K 9/15 column (GE Healthcare). By using gravity flow, the resin-bound protein was washed with 20 column volumes of the lysate buffer. The protein was then eluted in the same buffer supplemented with

10 mM maltose, and 10 mL fractions were collected. Fractions containing purified material were assessed by SDS/PAGE (12%). The purified protein contains two lower molecular weight bands that are both immunoreactive with anti-MBP antibody, suggesting that they are truncation products produced during overexpression (Fig. S3). The full-length protein is the most abundant band and consists of more than 60% of the total protein content. The first three fractions were concentrated to 3 mL with Amicon Ultra-15 Centrifugal Filter units (Millipore) and stored at −20 °C in the presence of 30% glycerol. The concentration was determined by using the appropriate extinction coefficient at a UV absorbance of 280 nm. The calculated protein concentration overestimated the amount of full-length protein, as a result of the presence of truncation products.

In Vitro Radioactivity-Based Assay. The ability of PglH to transfer UDP-Glc, UDP-Gal, UDP-GlcNAc, UDP-GalNAc, and GDP-Man was analyzed by using a radioactivity-based assay. To separate the radiolabeled Und-PP-disaccharide from excess of the labeled NDP sugars, the reactions were quenched in organic solvent, which allows for extraction of the hydrophobic undecaprenyl substrate. Repeated aqueous washes removed all of the excess aqueous-soluble NDP sugar.

The assays contained 3% DMSO, 0.05% dodecyl maltoside, 50 mM $MgCl_2$, 30 mM Tris-acetate, pH 8.0, 10 μM Und-PP-diNAcBac, 2 μM NDP sugar (20 mCi/mmol), 9 μM MBP-PglH, and water to a final volume of 100 μL. Und-PP-diNAcBac was prepared biosynthetically as previously described (12, 13). The reactions were initiated by the addition of enzyme and were monitored by quenching 15-μL aliquots at 2, 4, 6, 8, and 10 min into 1 mL of 2:1 chloroform:methanol and washing three times with 400 μL of an aqueous mixture composed of 1.83 g of potassium chloride dissolved in 235 mL water, 240 mL chloroform, and 15 mL methanol. The radioactivity present in the organic and aqueous layers was detected by using a LS6500 scintillation counter (Beckman); organic samples were dried and resuspended in 200 μL Solvable (Perkin-Elmer) and 5 mL of scintillation fluid (Opti-Fluor; Perkin-Elmer). Aqueous samples were mixed with 5 mL of Ecolite (MP Biomedicals) before counting. The assays with each sugar were performed in triplicate.

To prepare Und-PP-diNAcBac-Glc, the product of PglH, for subsequent labeling with fluorescent 2-AB, the reaction was performed in the absence of radiolabeled substrate. The reaction contained 3% DMSO, 0.1% DDM, 50 mM $MgCl_2$, 30 mM Tris (pH 8.0), 20 μM Und-PP-diNAcBac, 20 μM UDP-Glc, 10 μM PglH, and water to a final volume of 100 μL. The disaccharide was cleaved from the polyprenol and labeled with 2-AB as described previously (14). The labeling reaction was cleaned with GlycoClean S Cartridges (Prozyme) before purification using the normal phase GlycoSep N HPLC column (Prozyme) following previously established protocols (14). MALDI MS was used to verify the identity of the purified 2-AB–labeled disaccharide product (Fig. S3).

1. Freitag NE, Seifert HS, Koomey M (1995) Characterization of the *pilF-pilD* pilus-assembly locus of *Neisseria gonorrhoeae*. *Mol Microbiol* 16:575–586.
2. Aas FE, et al. (2006) *Neisseria gonorrhoeae* type IV pili undergo multisite, hierarchical modifications with phosphoethanolamine and phosphocholine requiring an enzyme structurally related to lipopolysaccharide phosphoethanolamine transferases. *J Biol Chem* 281:27712–27723.
3. Aas FE, Vik A, Vedde J, Koomey M, Egge-Jacobsen W (2007) *Neisseria gonorrhoeae O*-linked pilin glycosylation: Functional analyses define both the biosynthetic pathway and glycan structure. *Mol Microbiol* 65:607–624.
4. Robertson BD, Frosch M, van Putten JP (1993) The role of *galE* in the biosynthesis and function of gonococcal lipopolysaccharide. *Mol Microbiol* 8:891–901.
5. Hegge FT, et al. (2004) Unique modifications with phosphocholine and phosphoethanolamine define alternate antigenic forms of *Neisseria gonorrhoeae* type IV pili. *Proc Natl Acad Sci USA* 101:10798–10803.
6. Johnston DM, Cannon JG (1999) Construction of mutant strains of *Neisseria gonorrhoeae* lacking new antibiotic resistance markers using a two gene cassette with positive and negative selection. *Gene* 236:179–184.
7. Børud B, et al. (2010) Genetic, structural, and antigenic analyses of glycan diversity in the *O*-linked protein glycosylation systems of human *Neisseria* species. *J Bacteriol* 192: 2816–2829.
8. Mehr IJ, Long CD, Serkin CD, Seifert HS (2000) A homologue of the recombination-dependent growth gene, *rdgC*, is involved in gonococcal pilin antigenic variation. *Genetics* 154:523–532.
9. Mehr IJ, Seifert HS (1998) Differential roles of homologous recombination pathways in *Neisseria gonorrhoeae* pilin antigenic variation, DNA transformation and DNA repair. *Mol Microbiol* 30:697–710.
10. Chambers RE, Clamp JR (1971) An assessment of methanolysis and other factors used in the analysis of carbohydrate-containing materials. *Biochem J* 125:1009–1018.
11. Barsett H, Smestad Paulsen B (1992) Separation, isolation and characterization of acidic polysaccharides from the inner bark of *Ulmus glabra* Huds. *Carbohydr Polym* 17:137–144.
12. Glover KJ, Weerapana E, Imperiali B (2005) *In vitro* assembly of the undecaprenylpyrophosphate-linked heptasaccharide for prokaryotic *N*-linked glycosylation. *Proc Natl Acad Sci USA* 102:14255–14259.
13. Olivier NB, Chen MM, Behr JR, Imperiali B (2006) *In vitro* biosynthesis of UDP-N,N′-diacetylbacillosamine by enzymes of the *Campylobacter jejuni* general protein glycosylation system. *Biochemistry* 45:13659–13669.
14. O'Reilly MK, Zhang G, Imperiali B (2006) *In vitro* evidence for the dual function of Alg2 and Alg11: essential mannosyltransferases in *N*-linked glycoprotein biosynthesis. *Biochemistry* 45:9593–9603.
15. Chaudhuri RR, Pallen MJ (2006) xBASE, a collection of online databases for bacterial comparative genomics. *Nucleic Acids Res* 34(Database issue):D335–D337.
16. Thompson JD, Higgins DG, Gibson TJ (1994) CLUSTAL W: Improving the sensitivity of progressive multiple sequence alignment through sequence weighting, position-specific gap penalties and weight matrix choice. *Nucleic Acids Res* 22: 4673–4680.

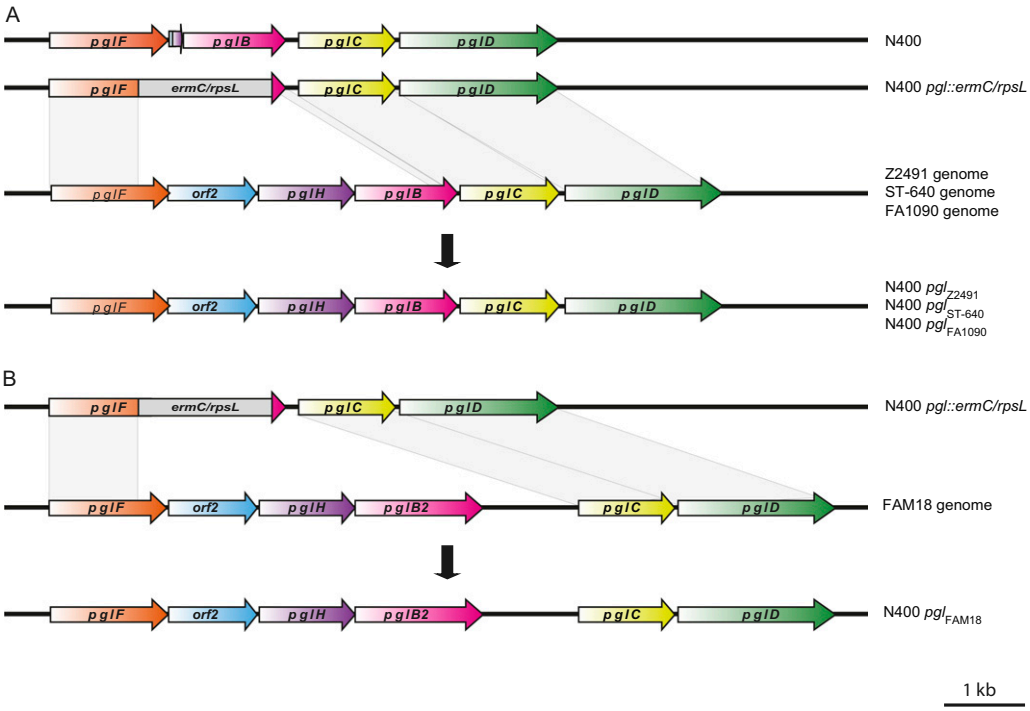

Fig. S1. Strategy for construction of strains with variant *pgl* loci. Different *pgl* loci were introduced into strain N400 (and its derivative 4/3/1) by using a two-step allelic exchange strategy that allowed gene replacement. The method uses a gene cassette containing both a selectable marker (*ermC′*) and a counter-selectable marker (*rpsL*$^{+}$) (6, 7). Genomic DNA from strains of interest was used to transform the recipient, selecting for streptomycin resistance and scoring for sensitivity to erythromycin. (*A*) The Z2491, ST-640, and FA1090 *pgl* loci all have the *pglB* allele (in addition to ORFs 2 and 3), (*B*) whereas the FAM18 *pgl* locus has the *pglB2* allele (and therefore synthesizes GATDH rather than diNAcBac-based glycoforms). The gray shaded area indicates regions allowing homologous recombination.

A

	pgl background			
Core Locus	wt	*pglA*	*pglH*	*pglA, pglH*
Ng N400	diNAcBac-AcHex	diNAcBac		
Nm Z2491	diNAcBac-AcHex	diNAcBac-AcHex	diNAcBac-AcHex	diNAcBac
Nl ST-640	diNAcBac-AcHex	diNAcBac-AcHex	diNAcBac-AcHex	diNAcBac
Ng FA1090	diNAcBac-AcHex	diNAcBac	diNAcBac-AcHex	diNAcBac
Nm FAM18	GATDH-AcHex†	GATDH / GATDH-AcHex*†	GATDH-AcHex	GATDH

B

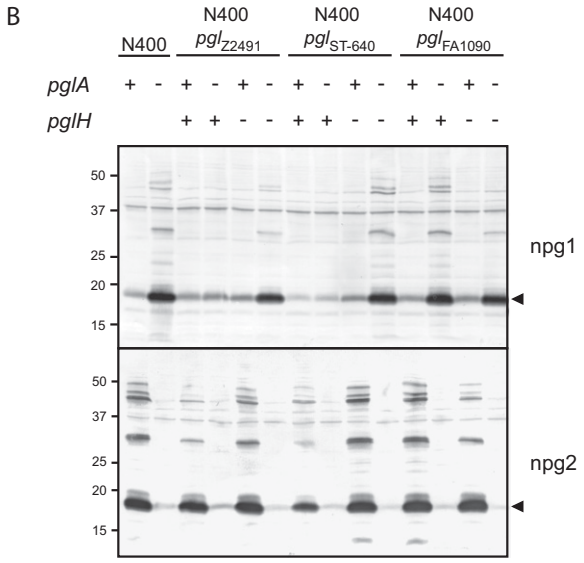

Fig. S2. The *pglH* gene is associated with altered disaccharide glycan composition. (*A*) ESI MS analysis of intact PilE were carried out to characterize the glycan structure (Fig. 2 and Table 1). The table summarizes different glycan forms synthesized by strains with various *pgl* backgrounds. *Ng, N. gonorrhoeae, Nm, N. meningitidis, Nl, N. lactamica*; *Mixture of mono- and disaccharide glycoforms. †Reduced acetylation. (*B*) Immunoblotting of whole-cell lysates from isogenic strains with different *pgl* backgrounds used glycan-specific monoclonal antibodies npg1 and npg2, recognizing diNAcBac monosaccharide and diNAcBac-Gal disaccharide glycoforms, respectively (7). As shown for the controls (two leftmost lanes) using strain N400 (that expresses PglA but lacks *pglH*), glycoproteins react with npg2 (indicative of diNAcBac-Gal modification). Inactivation of *pglA* in that background leads to a loss of npg2 reactivity and gain of npg1 reactivity (indicative of diNAcBac monosaccharide modification). Inactivation of *pglA* in backgrounds carrying active alleles of *pglH* fails to engender npg1 reactivity, thus indicating the absence of the diNAcBac monosaccharide modification. This phenotype is directly caused by PglH, as inactivation of *pglH* restored npg1 reactivity in these backgrounds. Moreover, strains expressing the PglH-associated disaccharide fail to react with npg2. Strains expressing active forms of PglA reacted with npg2, whereas strains in which *pglA* was mutated failed to react with mono- or disaccharide-specific antibodies, demonstrating that PglH is responsible for an antigenically different disaccharide than PglA. Consistent with its inactivity in disaccharide synthesis as seen by MS, the *pglH*$_{FA1090}$ allele is not associated with this phenotype. Minus signs denote *pglA*::*kan* or *pglH*::*ermC/rpsL*; plus signs denote intact *pglA* or *pglH*. Strains used are KS100 (N400), KS141 (N400 *pglA*), KS369 (N400 *pgl*$_{Z2491}$), KS370 (N400 *pgl*$_{Z2491}$ *pglA*), KS371 (N400 *pgl*$_{Z2491}$ *pglH*), KS372 (N400 *pgl*$_{Z2491}$ *pglA pglH*), KS351 (N400 *pgl*$_{ST-640}$), KS352 (N400 *pgl*$_{ST-640}$ *pglA*), KS353 (N400 *pgl*$_{ST-640}$ *pglH*), KS354 (N400 *pgl*$_{ST-640}$ *pglA pglH*), KS378 (N400 *pgl*$_{FA1090}$), KS379 (N400 *pgl*$_{FA1090}$ *pglA*), KS380 (N400 *pgl*$_{FA1090}$ *pglH*), and KS381 (N400 *pgl*$_{FA1090}$ *pglA pglH*). Arrow denotes the position of the major glycoprotein PilE.

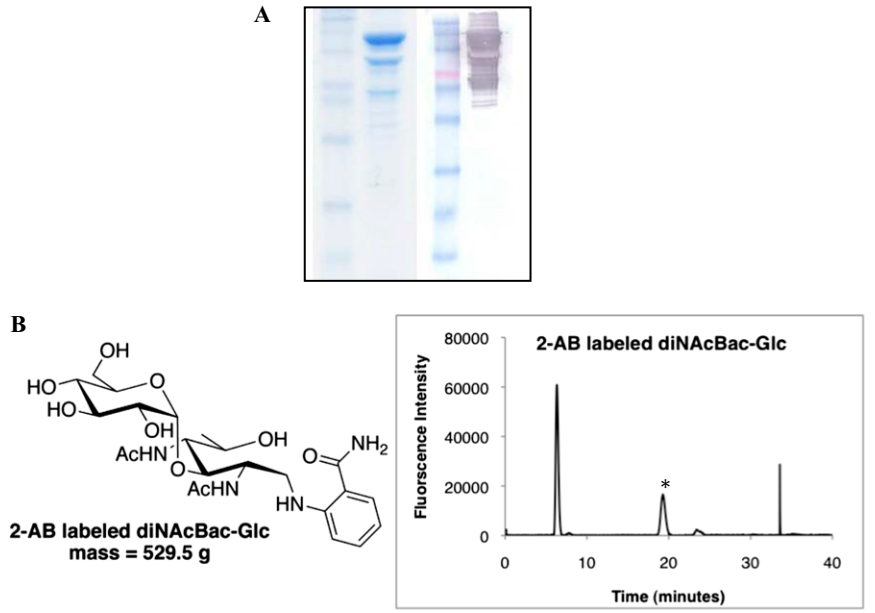

Fig. S3. (*A*) Characterization of the purified, recombinant MBP-PglH fusion protein. In SDS/PAGE (*Left*) and immunoblot (*Right*) analyses, the uppermost band corresponds to the molecular weight of the MBP-PglH construct and is the predominant protein band in the sample. MBP antibody was used to confirm the presence of the fusion tag MBP appended to PglH. Other bands also reacted with the MBP antibody and represent truncation products accumulated during expression. The Benchmark Pre-Stained Protein Ladder (Invitrogen) was used as a standard in the first lane. (*B*) Normal phase HPLC with fluorescence detection of 2-AB–labeled diNAcBac-Glc. To confirm that the product of PglH is diNAcBac-Glc, the glycan was hydrolyzed from the undecaprenyl-pyrophosphate linker and labeled with 2-AB. The diNAcBac-Glc retention time (asterisk) is consistent with other disaccharides, and MALDI MS confirmed the identity of the separated fluorescent product.

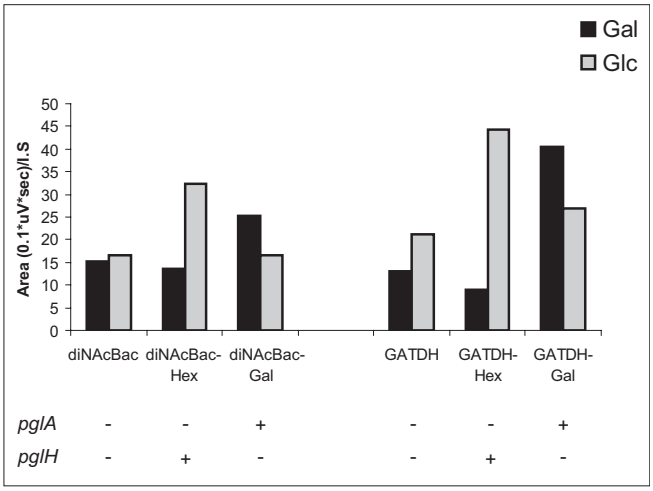

Fig. S4. Monosaccharide analyses are consistent with the finding that PglH transfers glucose to diNAcBac and GATDH. Relative amounts of galactose and glucose associated with purified pili as determined by gas chromatography after methanolysis and trimethylsilyl derivatization. Strains used are KS372 (N400 pgl_{Z2491} *pglA pglH*), KS370 (N400 pgl_{Z2491} *pglA*), and KS371 (N400 pgl_{Z2491} *pglH*) to synthesize diNAcBac, diNAcBac-Glc, and diNAcBac-Gal, respectively. KS363 (N400 pgl_{FAM18} *pglA pglH*), KS361 (N400 pgl_{FAM18} *pglA*), and KS362 (N400 pgl_{FAM18} *pglH*) synthesize GATDH, GATDH-Glc, and GATDH-Gal, respectively. The results are presented as the area under peak (0.1*uV*s) relative to the internal standard mannitol run together with each sample.

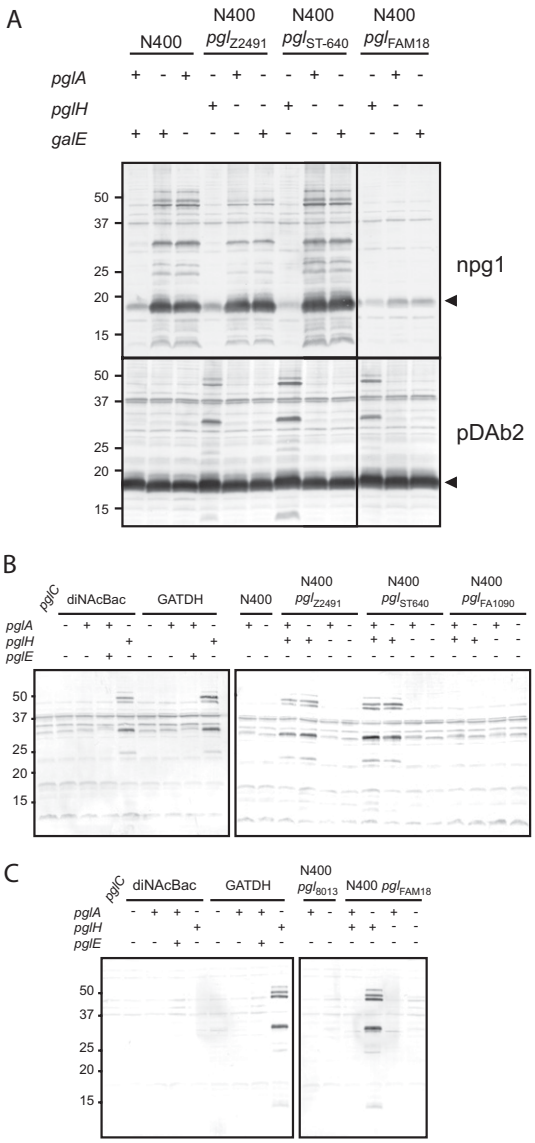

Fig. S5. (*A*) *galE* is epistatic to *pglA* but not to *pglH*. Immunoblotting of whole-cell lysates from isogenic strains with different *pgl* backgrounds used the glycan-specific monoclonal antibody npg1 and the polyclonal pDAb2 antibody, recognizing diNAcBac monosaccharide and diNAcBac-Glc disaccharide glycoforms, respectively. Minus signs denote *pglA*::*kan*, *pglH*::*ermC*/*rpsL* or *galE*::*cat*. Plus signs denote intact *pglA*, *pglH*, or *galE*. Note that inactivation of *galE* in N400 leads to glycoprotein reactivity with npg1 despite the presence of active *pglA*, whereas it has no effect on glycoprotein reactivity with the pDAb2 antibody in the strains expressing *pglH*. Strains used are KS100 (N400), KS141 (N400 *pglA*), KS442 (N400 *galE*), KS374 (N400 pgl_{Z2491} *pglA galE),* KS375 (N400 pgl_{Z2491} *pglH galE*), KS372 (N400 pgl_{Z2491} *pglA pglH*), KS356 (N400 pgl_{ST-640} *pglA galE*), KS357 (N400 pgl_{ST-640} *pglH galE*), KS354 (N400 pgl_{ST-640} *pglA pglH*), KS365 (N400 pgl_{FAM18} *pglA galE),* KS366 (N400 pgl_{FAM18} *pglH galE*), and KS363 (N400 pgl_{FAM18} *pglA pglH*). Arrow points to the major glycoprotein PilE. (*B*, *C*) PglH-derived disaccharides are uniquely immunogenic and antigenic. (*B*) Immunoblots of whole cell-lysates from strains with defined *pgl* backgrounds were probed with pDAb2, polyclonal antiserum raised against pili bearing the PglH-derived disaccharide diNAcBac-Glc. pDAb2 reactivity was specific to both PglH-derived glycans, diNAcBac-Glc and GATDH-Glc. Minus signs denote *pglA*::*kan*, *pglH*::*ermC*/*rpsL* or $pglE_{off}$. Plus signs denote intact *pglA*, *pglH*, or $pglE_{on}$. A *pglC*-null mutant was used as a negative control (far left lane). The strains used were (*Left*) KS105 (4/3/1 *pglC*), KS122 (4/3/1 *pglA*), KS101 (4/3/1), KS127 (4/3/1 $pglE_{on}$), KS400 (N400 pgl_{Z2491}, *pglA pilE*), KS312 (4/3/1 $pglB2_{8013}$ *pglA*), KS311 (4/3/1 $pglB2_{8013}$), KS310 (4/3/1 $pglB2_{8013}$ $pglE_{on}$), and KS394 (N400 pgl_{FAM18} *pglA, pilE*); and (*Right*) KS101 (4/3/1), KS122 (4/3/1 *pglA*), KS399 (N400 pgl_{Z2491} *pilE*), KS400 (N400 pgl_{Z2491} *pglA pilE*), KS401 (N400 pgl_{Z2491} *pglH pilE*), KS402 (N400 pgl_{Z2491} *pglA pglH pilE*), KS387 (N400 pgl_{ST-640} *pilE*), KS388 (N400 pgl_{ST-640} *pglA pilE*), KS389 (N400 pgl_{ST-640} *pglH pilE*), KS390 (N400 pgl_{ST-640} *pglA pglH pilE*), KS405 (N400 pgl_{FA1090} *pilE*), KS406 (N400 pgl_{FA1090} *pglA pilE*), KS407 (N400 pgl_{FA1090} *pglH pilE*), and KS408 (N400 pgl_{FA1090} *pglA pglH pilE*). (*C*) Immunoblots of whole-cell lysates from strains with defined *pgl* backgrounds were probed with pGAb2, polyclonal antiserum raised against pili bearing the PglH-derived disaccharide GATDH-Glc. pGAb2 reactivity was specific to strains expressing PglB2 and PglH. Minus signs denote *pglA*::*kan, pglH*::*ermC*/*rpsL* or $pglE_{off}$. Plus signs denote intact *pglA*, *pglH*, or *pglE*. A *pglC*-null mutant was used as a negative control (far left lane). Strains used were (*Left*) KS105 (4/3/1 *pglC*), KS122 (4/3/1 *pglA*), KS101 (4/3/1), KS127 (4/3/1 $pglE_{on}$), KS400 (N400 pgl_{Z2491}, *pglA pilE*), KS312 (4/3/1 $pglB2_{8013}$ *pglA*), KS311 (4/3/1 $pglB2_{8013}$), KS310 (4/3/1 $pglB2_{8013}$ $pglE_{on}$), and KS394 (N400 pgl_{FAM18} *pglA, pilE*); and (*Right*) KS311 (4/3/1 $pglB2_{8013}$), KS312 (4/3/1 $pglB2_{8013}$ *pglA*), KS393 (N400 pgl_{FAM18} *pilE*), KS394 (N400 pgl_{FAM18} *pglA pilE*), KS395 (N400 pgl_{FAM18} *pglH pilE*), and KS396 (N400 pgl_{FAM18} *pglA pglH pilE*).

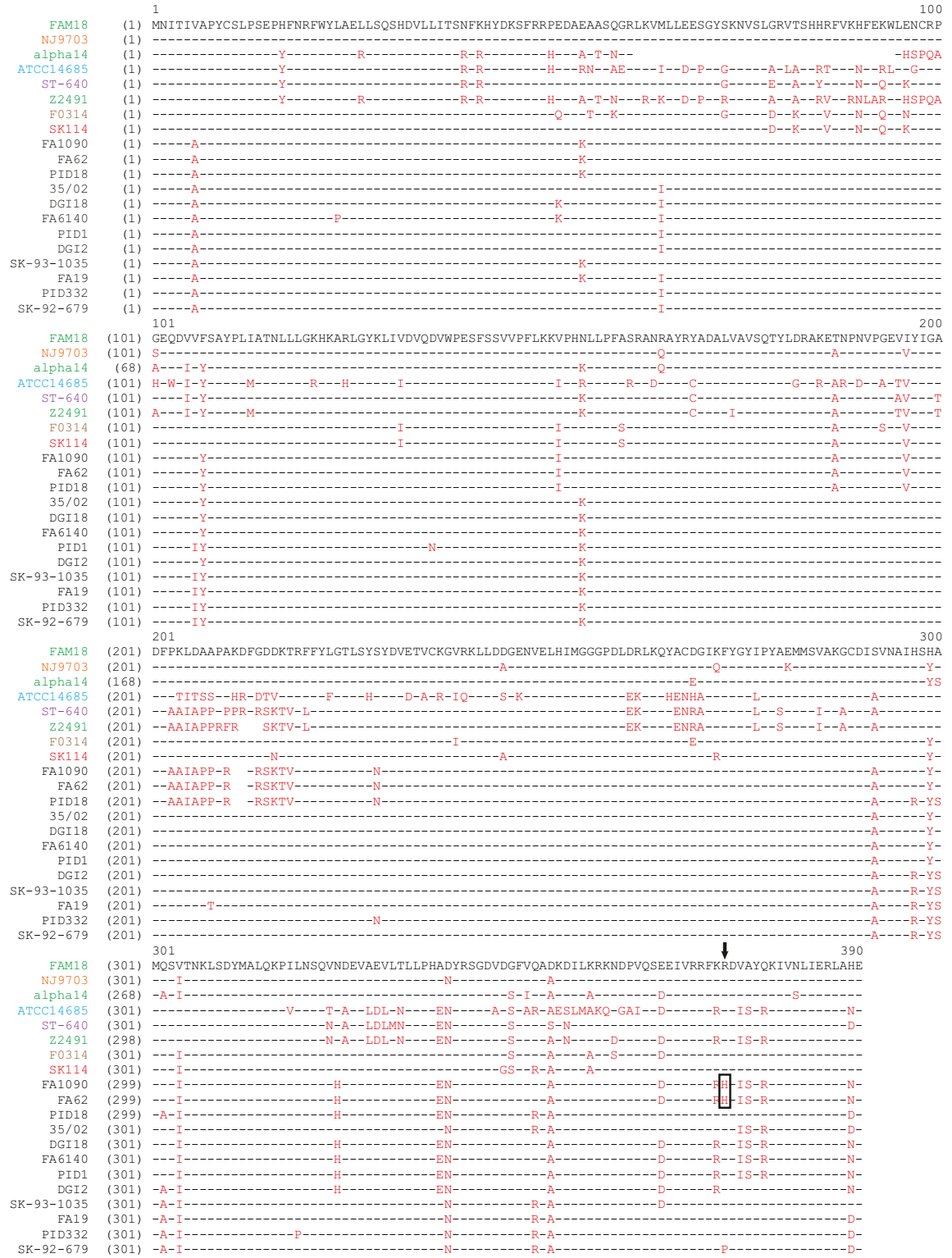

Fig. S6. Amino acid sequence alignment of PglH proteins. PglH from strain FAM18 was used as consensus sequence. Amino acid differences are shown in red and identical amino acids are represented by minus signs. The critical amino acid, histidine 371, in FA1090 is boxed. National Center for Biotechnology Information protein accession numbers are shown in parentheses: *N. gonorrhoeae* strains (shown in black) 35/02 (ZP_06128240.1), DGI18 (ZP_04720314.1), DGI2 (ZP_06570304.1), FA1090 (YP_207259.1), FA62 (ZP 06641922.1), FA19 (ZP_06130290.1), FA6140 (ZP_04722383.1), PID1 (ZP_06137079.1), PID18 (ZP_06134762.1), PID332 (ZP_06148242.1), SK-92–679 (ZP_06150409.1), SK-93–1035 (ZP_06152714.1); *N. meningitidis* strains (shown in green) alpha14 (YP_003082587.1), FAM18 (YP_974510.1), Z2491 (YP_002342109.1), *Neisseria cinerea* ATCC 14685 (shown in blue; ZP_05982849.1), *Neisseria* sp. oral taxon 014 str. F0314 (shown in brown; ZP_06981261.1), *N. subflava* NJ9703 (shown in orange; ZP_05985778.1), *Neisseria flavescens* SK114 (shown in red; ZP_04757589.1), and *N. lactamica* ST-640 [shown in purple; named NLA17570 in xBASE (15)]. Alignment was made with AlignX in Vector NTI Advance 11 (Invitrogen) that uses a modified ClustalW algorithm (16).

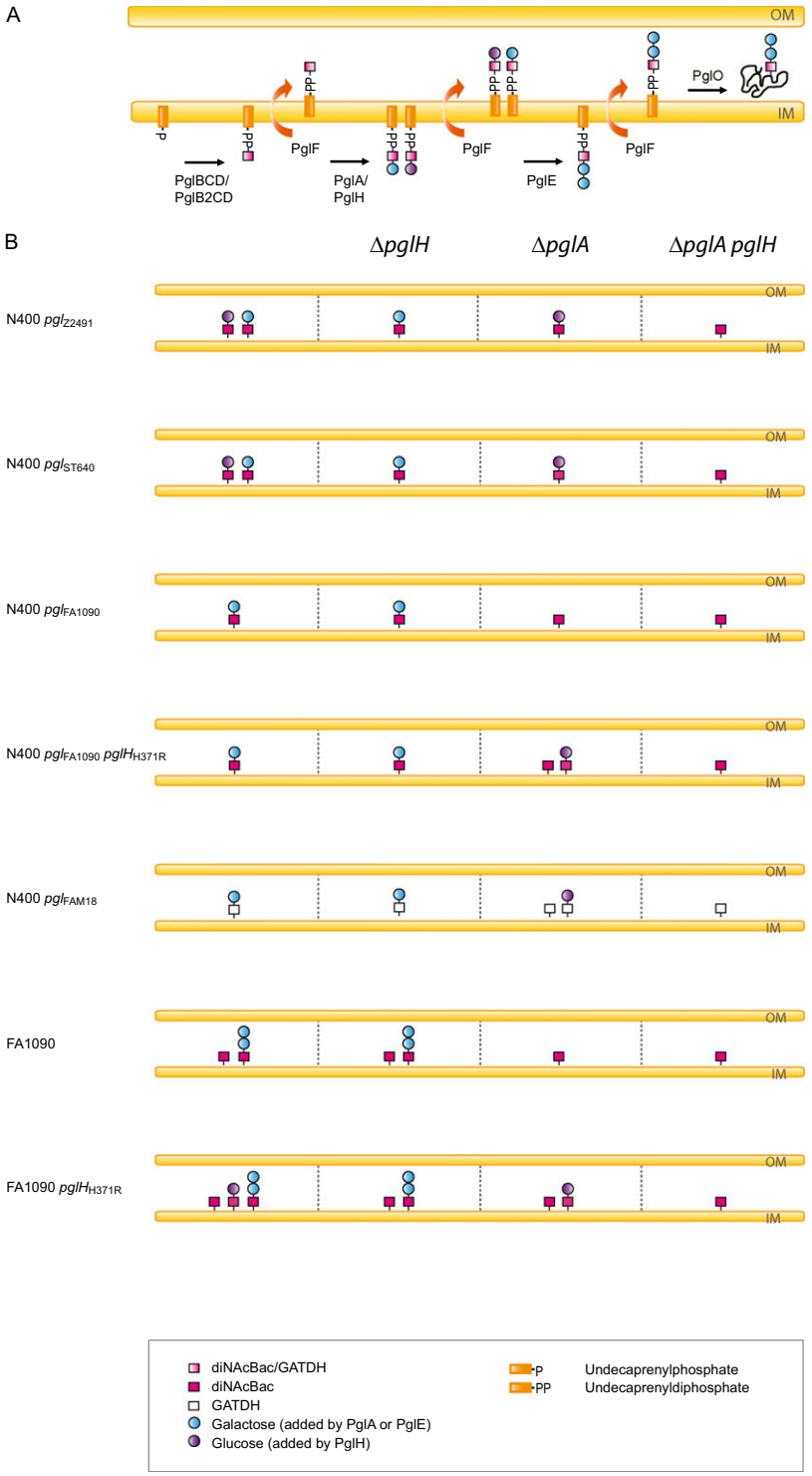

Fig. S7. (*A*) Revised *O*-linked protein glycosylation pathway in *Neisseria* species including the PglH glucosyltransferase. (*B*) Influence of select *pglA* and *pglH* alleles on glycoform expression in defined genetic backgrounds. Shown are the UndPP-associated glycoforms expressed in each instance.

Table S1. *Neisseria* strains and *pgl* genotypes

Strain	Accession no.	*orf2*	*pglH*	*pglA*	*pglE*	*pglB*	Origin
N. gonorrhoeae							
FA1090	NC_002946.2	ON	ON	ON	ON (-PV)	*pglB*	DGI
F62	ADAA01000005.1	ON	ON	ON (-PV)	ON (-PV)	*pglB*	UI
PID1	ABZM01000034.1	OFF	ON (-PV)	ON (-PV)	OFF	*pglB*	PID
FA6140	ABZI01000024.1	OFF	ON (-PV)	OFF	ON	*pglB*	ES
PID24-1	ABZN01000022.1	OFF	ON (-PV)	OFF	OFF	*pglB*	PID
DGI18	ABZH01000024.1	OFF	ON (-PV)	OFF	OFF	*pglB*	DGI
PID332	ABZO01000041.1	OFF	ON	ON (-PV)	OFF	*pglB*	PID
35/02	ABZG01000029.1	OFF	ON (-PV)	ON (-PV)	OFF	*pglB*	
SK-93–1035	ABZQ01000041.1	ON	ON (-PV)	OFF	OFF	*pglB*	DGI
SK-92–679	ABZP01000038.1	OFF	ON (-PV)	ON	OFF	*pglB*	DGI
FA19	ABZJ01000029.1	OFF	ON (-PV)	OFF	OFF	*pglB*	UI
PID18	ABZL01000024.1	OFF	ON	ON (-PV)	OFF	*pglB*	PID
DGI2	ACIG01000103.1	OFF	ON (-PV)	ON (-PV)	OFF	*pglB*	DGI
MS11	ABZK01000025.1	—	—	ON (-PV)	OFF	*pglB*	UI
NCCP11945	NC_011035.1	—	—	ON (-PV)	OFF	*pglB*	
1291	ABZF01000025.1	—	—	ON (-PV)	OFF	*pglB*	GU
N. lactamica							
ST-3787/ATCC 23970	ACEQ02000033.1	OFF	OFF	ON	ON	*pglB*	C
ST-640	NC_014752.1	OFF	ON	OFF	ON	*pglB*	C
Y92-1009	CACL01000022.1	OFF	ON	ON	OFF	*pglB*	C
NS19	AEPI01000013.1	OFF	OFF	OFF	OFF	*pglB*	C
N. meningitidis							
H44/76	AEQZ01000037.1	—	—	ON	OFF	*pglB*	IMD
MC58	NC_003112.2	—	—	ON	OFF	*pglB*	IMD
ATCC 13091	AEEF01000085.1	ON	OFF	OFF	OFF	*pglB*	
K1207	ADWM01000120.1	OFF	ON (-PV)	ON	OFF	*pglB2*	IMD
S0108	ADWN01000126.1	ON	ON (-PV)	OFF	OFF	*pglB2*	IMD
Z2491	NC_003116.1	OFF	ON	ON	ON	*pglB*	IMD
053442	NC_010120.1	ON	OFF	ON	OFF	*pglB2*	IMD
NS44	AEPJ01000151.1	ON	OFF	ON	OFF	*pglB2*	
FAM18	NC_008767.1	OFF	ON (-PV)	OFF	OFF	*pglB2*	IMD
ALPHA14	NC_013016.1	OFF	ON (-PV)	ON	OFF	*pglB*	HC
8013	FM999788	—	—	OFF	OFF	*pglB2*	IMD
M6190	AEQF01000040.1	OFF	ON (-PV)	ON	OFF	*pglB2*	IMD
ES14902	AEQI01000038.1	OFF	ON (-PV)	ON	OFF	*pglB2*	IMD
M0579	AEQH01000026.1	OFF	OFF	OFF	OFF	*pglB2*	IMD
OX99.30304	AEQE01000110.1	OFF	OFF	OFF	OFF	*pglB2*	HC
961–5945	AEQK01000132.1	ON	ON	ON	ON	*pglB2*	IMD
M13399	AEQG01000039.1	—	—	ON	OFF	*pglB*	IMD
N1568	AEQD01000080.1	—	—	OFF	OFF	*pglB2*	IMD
CU385	AEQJ01000044.1	—	—	ON	OFF	*pglB*	IMD
M01-240013	AEQL01000047.1	—	—	OFF	ON	*pglB*	IMD
N. flavescens NRL30031/H210	ACEN01000095.1	ON	OFF	—	—	*pglB*	C
N. flavescens SK114	ACQV01000018.1	ON	ON (-PV)	—	—	*pglB2*	C
Neisseria subflava NJ9703	ACEO02000013.1	ON	ON (-PV)	—	—	*pglB2*	C
Neisseria mucosa C102	ACRG01000017.1	ON	ON (-PV)	—	—	*pglB2*	C
Neisseria mucosa ATCC 25996	ACDX02000011.1	ON	ON (-PV)	—	—	*pglB2*	C
Neisseria sicca DS1	AEPG01000397.1	ON	ON (-PV)	—	—	*pglB2*	C
Neisseria sicca 4320	AEPF01000056.1	ON	ON (-PV)	—	—	*pglB2*	C
Neisseria sicca ATCC 29256	ACKO02000014.1	ON	ON (-PV)	—	—	*pglB2*	C
Neisseria polysaccharea NS342	AEPH01000240.1	ON	ON (-PV)	—	OFF	*pglB*	C
Neisseria polysaccharea ATCC 43768	ADBE01000085.1	—	—	OFF	ON	*pglB*	C
N. cinerea ATCC 14685	ACDY02000005.1	ON	ON (-PV)	—	—	*pglB*	C
Neisseria sp. oral taxon 014 str. F0314	ADEA01000027.1	ON	ON (-PV)	—	—	*pglB2*	C
Neisseria elongata subsp. glycolytica ATCC 29315	ADBF01000031.1	ON	OFF	—	—	*pglB*	C
Neisseria bacilliformis ATCC BAA-1200	AFAY01000015.1	ON	ON (-PV)	—	—	*pglB*	C

C, commensal strain; DGI, disseminated Gonococcal infection; ES, epidemic strain; GU; Gonococcal urethritis; HC, healthy carrier; IMD, invasive Meningococcal disease; PID, pelvic inflammatory disease; UI, uncomplicated infection; (-PV), not phase variable.

Table S2. Complete list of PilE modifications and corresponding masses *m/z*

Modifications present	MW of PilE, Da*	Modifications present	MW of PilE, Da*
None	17,179[†]	—	—
1PE	17,302	—	—
2PE	17,425	—	—
diNAcBac	17,407	GATDH	17,453
diNAcBac- Hex	17,569	GATDH-Hex	17,615
diNAcBac-GalNAc	17,610	GATDH-GalNAc	17,656
diNAcBac-AcHex	17,611	GATDH-AcHex	17,657
diNAcBac-AcGalNAc	17,652	GATDH-AcGalNAc	17,698
diNAcBac-HexHex	17,732	GATDH-HexHex	17,778
diNAcBac-HexGalNAc	17,773	GATDH-HexGalNAc	17,819
diNAcBac-HexAcHex	17,774	GATDH-HexAcHex	17,820
diNAcBac-HexAcGalNAc	17,815	GATDH-HexAcGalNAc	17,861
1PE, diNAcBac	17,530	1PE, GATDH	17,576
1PE, diNAcBac- Hex	17,692	1PE, GATDH-Hex	17,738
1PE, diNAcBac-GalNAc	17,733	1PE, GATDH-GalNAc	17,779
1PE, diNAcBac-AcHex	17,734	1PE, GATDH-AcHex	17,780
1PE, diNAcBac-AcGalNAc	17,775	1PE, GATDH-AcGalNAc	17,821
1PE, diNAcBac-HexHex	17,855	1PE, GATDH-HexHex	17,901
1PE, diNAcBac-HexGalNAc	17,896	1PE, GATDH-HexGalNAc	17,942
1PE, diNAcBac-HexAcHex	17,897	1PE, GATDH-HexAcHex	17,943
1PE, diNAcBac-HexAcGalNAc	17,938	1PE, GATDH-HexAcGalNAc	17,984
2PE, diNAcBac	17,653	2PE, GATDH	17,699
2PE, diNAcBac-Hex	17,815	2PE, GATDH-Hex	17,861
2PE, diNAcBac-GalNAc	17,856	2PE, GATDH-GalNAc	17,902
2PE, diNAcBac-AcHex	17,857	2PE, GATDH-AcHex	17,903
2PE, diNAcBac-AcGalNAc	17,898	2PE, GATDH-AcGalNAc	17,944
2PE, diNAcBac-HexHex	17,978	2PE, GATDH-HexHex	18,024
2PE, diNAcBac-HexGalNAc	18,019	2PE, GATDH-HexGalNAc	18,065
2PE, diNAcBac-HexAcHex	18,020	2PE, GATDH-HexAcHex	18,066
2PE, diNAcBac-HexAcGalNAc	18,061	2PE, GATDH-HexAcGalNAc	18,107
	m/z of oxonium ion		*m/z* of oxonium ion
diNAcBac	229.1	GATDH	275.2
Ac2GalNAc	288.2	Ac2GalNAc	—
diNAcBac-Hex	391.1	GATDH-Hex	437.2
diNAcBac-GalNAc	432.2	GATDH-GalNAc	—
diNAcBac-AcHex	433.2	GATDH-AcHex	479.2
diNAcBac-AcGalNAc	474.2	GATDH-AcGalNAc	—
diNAcBac-Ac2GalNAc	516.2	GATDH-Ac2GalNAc	—
diNAcBac-HexHex	553.2	GATDH-HexHex	—
diNAcBac-HexGalNAc	594.2	GATDH-HexGalNAc	—
diNAcBac-HexAcHex	595.2	GATDH-HexAcHex	—
	636.2	GATDH-HexAcGalNAc	

Hex, hexose; GalNAc,*N*-acetyl galactosamine; Ac, acetyl-group.

*Detected or expected molecular weight in ESI MS.

[†]Calculated theoretical molecular weight of 17,178.5 (including one intramolecular disulfide bridge).